

International Journal of Geographical Information Science

Publication details, including instructions for authors and subscription information:

<http://www.tandfonline.com/loi/tgis20>

Measuring the temporal instability of land change using the Flow matrix

D. S.M. Runfola^a & R. G. Pontius Jr.^b

^a National Center for Atmospheric Research, Institute of Behavioral Science, Colorado University, Boulder, CO USA

^b Graduate School of Geography, Clark University, Worcester, MA, USA

Published online: 14 Jun 2013.

To cite this article: D. S.M. Runfola & R. G. Pontius Jr. (2013) Measuring the temporal instability of land change using the Flow matrix, International Journal of Geographical Information Science, 27:9, 1696-1716, DOI: [10.1080/13658816.2013.792344](https://doi.org/10.1080/13658816.2013.792344)

To link to this article: <http://dx.doi.org/10.1080/13658816.2013.792344>

PLEASE SCROLL DOWN FOR ARTICLE

Taylor & Francis makes every effort to ensure the accuracy of all the information (the "Content") contained in the publications on our platform. However, Taylor & Francis, our agents, and our licensors make no representations or warranties whatsoever as to the accuracy, completeness, or suitability for any purpose of the Content. Any opinions and views expressed in this publication are the opinions and views of the authors, and are not the views of or endorsed by Taylor & Francis. The accuracy of the Content should not be relied upon and should be independently verified with primary sources of information. Taylor and Francis shall not be liable for any losses, actions, claims, proceedings, demands, costs, expenses, damages, and other liabilities whatsoever or howsoever caused arising directly or indirectly in connection with, in relation to or arising out of the use of the Content.

This article may be used for research, teaching, and private study purposes. Any substantial or systematic reproduction, redistribution, reselling, loan, sub-licensing, systematic supply, or distribution in any form to anyone is expressly forbidden. Terms & Conditions of access and use can be found at <http://www.tandfonline.com/page/terms-and-conditions>

Measuring the temporal instability of land change using the Flow matrix

D.S.M. Runfola^{a*} and R.G. Pontius Jr.^b

^aNational Center for Atmospheric Research, Institute of Behavioral Science, Colorado University, Boulder, CO USA; ^bGraduate School of Geography, Clark University, Worcester, MA, USA

(Received 5 March 2012; final version received 6 March 2013)

This article introduces the Flow matrix, which expresses the sizes of transitions among categories between two time points. We use the Flow matrix to create a metric R that measures the instability of annual change among time intervals that partition the time extent. Specifically, R is the proportion of change that would need to be reallocated to different time interval(s) to achieve uniform change during the time extent. This article computes R for 10 Long Term Ecological Research (LTER) sites and for seven case studies from published land change data. Of the 10 LTER sites analyzed, the Andrews site in Oregon had the highest R value (37.1% of change), while the Luquillo site in Puerto Rico had the lowest (1.7% of change). We analyze the mathematical behavior of R , especially with respect to how the partitioning of the time extent into intervals can influence R .

Keywords: temporal stability; model assumptions; land-change science; Markov; LTER

1. Introduction

1.1. Research objective

Land change has major implications for a broad range of phenomena, including deforestation, agriculture, and sustainability (Turner *et al.* 1995, Lambin *et al.* 2001, UN-REDD 2010). Investigation of the many factors that influence land cover and land use provides an avenue through which the human–environment interface can be better understood, and recent research has emphasized the need for a better understanding of how anthropogenic processes influence land change (Nagendra *et al.* 2004). The impact of land change on the vulnerability and sustainability of human-dominated landscapes has begun to be analyzed, and improvement of understanding is a major goal of parties interested in examining the consequences of land-use change (Foley *et al.* 2005, GLP 2010). Ongoing research into land-cover change modeling has called for the ability to measure the degree to which ‘change progression [is] constant in time’ (Lambin 1997, Petit *et al.* 2001, p. 3436, Pontius *et al.* 2007, Pontius and Neeti 2010, Aldwaik and Pontius 2012). In response to this need, this article explores the research question: *How can the temporal stability of land change be measured?*

*Corresponding author. Email: dan@danrunfola.com

1.2. Definitions

Our article uses three terms to describe periods of time: extent, interval, and duration. Extent is the period of time from the first date to the last date in a time series of data, e.g., 1970–2000. An interval is a period of time within the extent for which data exist both at an initial date and at a subsequent date, e.g., 1980–1990. Duration is the amount of time of any period within an extent, irrespective of data availability, e.g., three decades, one decade, or a single year. This article also uses the term temporal stability. Temporal stability, temporal stationarity, and temporal homogeneity have been used interchangeably to describe the degree to which the rate of land change is consistent over a given temporal extent (see Bell and Hinojosa 1977, Petit *et al.* 2001, Flamenco-Sandoval *et al.* 2007, Pontius *et al.* 2007, Pontius and Neeti 2010, Takada *et al.* 2010).

1.3. Literature review

Modeling and describing the process of land change across time is a frequent goal of land-change modelers. However, many basic challenges remain – from understanding path dependence (Caillault *et al.*, in Press, An and Brown 2008) to quantifying uncertainty and accuracy (Rindfuss *et al.* 2004, Pontius *et al.* 2007). One such basic challenge is to measure how consistent historic land change has been i.e., temporal stability, either to describe landscape dynamics or to calibrate a model for future projections. The concept of temporal stability has been applied to test the validity of model assumptions (Bell and Hinojosa 1977, Petit *et al.* 2001), to quantify the influence of uncertainty on future projections (Pontius and Neeti 2010), to explore change trajectories (Petit *et al.* 2001, An and Brown 2008), and to examine inter-interval rates of change (Takada *et al.* 2010).

Across each of these applications, temporal stability has been defined using various mathematical approaches. The basis of many approaches is the popular Markov chain model (Rindfuss *et al.* 2004, An and Brown 2008), which can be expressed as follows (Petit *et al.* 2001, Takada *et al.* 2010):

$$\mathbf{V}_{t+1} = \mathbf{V}_t \mathbf{M}_t \quad (1)$$

where \mathbf{V}_t is a 1-by- J row vector of land-cover proportions at time t , and J is the number of categories in the classification. \mathbf{M}_t is a J -by- J transition matrix for which each entry m_{ij} in the matrix is the conditional probability of transition of a patch of land from category i at the initial time t to category j at the subsequent time $t + 1$, given the patch is a member of category i at the initial time. In the Markov matrix, this conditional probability is calculated from the raw transition matrix, which is a J -by- J matrix in which each entry c_{ij} is the size, e.g., square meters, of the area that transitioned from category i at time t to category j at time $t + 1$. In the Markov approach, a single time interval is generally chosen for the calibration of matrix \mathbf{M}_t in order to make projections of future land change beyond the final observed year Y_T . The probability m_{ij} in the Markov approach is calculated by dividing entry c_{ij} of the raw matrix by the row's marginal sum in the raw matrix:

$$m_{ij} = \frac{c_{ij}}{\sum_{j=1}^J c_{ij}} \quad (2)$$

Using this Markov approach, perfect temporal stability, i.e., stationarity, is said to exist when matrix \mathbf{M}_t retains the same set of m_{ij} probabilities for all time intervals (Bell and

Hinojosa 1977, Petit *et al.* 2001, Flamenco-Sandoval *et al.* 2007). Stationarity is a critical assumption of Markov-based models of land-cover change, as Mertens and Lambin (2000) highlight:

When dealing with nonstationary processes, these [Markov] models lose any predictive ability unless one modifies the transitions probabilities through time according to some complex model design. . . (p. 481).

In theory, the stability of a system can be tested by deriving a Markov matrix for two time intervals and analyzing the differences between the matrices (Bell and Hinojosa 1977, Petit *et al.* 2001, Pueyo and Beguería 2007, Pelorosso *et al.* 2011). However, to make this comparison meaningful, the m_{ij} probabilities that make up each matrix \mathbf{M}_t must be adjusted to represent an equivalent duration, e.g., 1 year (Bell and Hinojosa 1977, Petit *et al.* 2001, Takada *et al.* 2010).

This adjustment is frequently an annualization of the Markov matrix that is traditionally performed by taking the n th power root, where n is the empirical duration of the original, unadjusted Markov matrix divided by the desired duration. Recent literature has also discussed alternative, diagonalization approaches (Flamenco-Sandoval *et al.* 2007). Takada *et al.* (2010) provide a comparison and analysis of these methods, and find that multiple solutions exist for some Markov matrices. For other Markov matrices, the only solutions contain negative or imaginary entries (Takada *et al.* 2010), and thus the entries cannot be interpreted as probabilities.

A variety of methods have been applied to determine whether a Markov matrix calculated based on one time interval is similar to a Markov matrix calculated based on a different time interval. Bell and Hinojosa (1977) propose using Pearson's goodness-of-fit statistic to compare two annualized Markov matrices, but they offer no guidance on how to interpret these results. Pueyo and Beguería (2007) and Pelorosso *et al.* (2011) utilize the Anderson–Goodman test (1957), which compares the matrix from a single time interval to a composite matrix for the entire time extent (Ellis 1979). Petit *et al.* (2001) adopt two strategies. First, they compare the equilibrium reached among land-cover categories when calibrating the Markov matrices with different intervals. Using their first approach, they found a different equilibrium for each calibration interval for their data, indicating a lack of stationarity. Second, they projected land change based on Markov matrices created from a limited subset of their data to test the agreement between projections and observed data for back-casting, forecasting, and interpolation. They drew the conclusion that 'the process of land-cover change does generally not conform to the hypothesis of stationarity and, therefore, Markov chain models provide unreliable projections' (p. 3455).

There are many situations where the assumptions of the Markov model are not appropriate or where alternative assumptions are equally valid. For example, the Markov model assumes that a constant proportion of the initial category transitions to other categories at each time step. Consequently, extrapolations over multiple time steps approach a state of equilibrium regarding the size of each category (Pettit *et al.* 2001). If all systems approached equilibrium, then we would not be facing the sustainability crisis that exists today.

To provide an alternative to the Markov matrix when either no interpretable solutions are available or the Markov assumptions are inappropriate, this article expands the study of temporal stability by using the Flow matrix. The term Flow matrix is drawn from models that represent stocks and flows of information, material, or energy during discrete time intervals (see Parker *et al.* 2003). In land change, stocks can be understood as persistent land, i.e., land that does not change, while flows are changes on the landscape. The Flow

matrix portrays a constant quantity of transition per time step (Pontius *et al.* 2004, Braimoh 2006, Aldwaik and Pontius 2012). This necessitates a measurement of temporal stability that focuses on a linear change in the system (c.f. Pontius *et al.* 2004, Braimoh 2006, Alo and Pontius 2008, Versace *et al.* 2008). Our article provides a measurement for temporal stability based on the Flow matrix.

2. Methods

2.1. Notation and definition of the Flow matrix

This article uses a Flow matrix to calculate temporal instability for 10 study sites. The Flow matrix is a $(J + 1)$ -by- $(J + 1)$ matrix, where J is the number of categories. The J -by- J matrix within the upper left of the Flow matrix contains entries that give the size of each categorical transition. The diagonal entries are not included because they indicate stocks, i.e., persistence, rather than flows, i.e., change. The final $(J + 1)^{\text{th}}$ column at the right and the final $(J + 1)^{\text{th}}$ row at the bottom are the totals, which give the gross losses and gross gains, respectively, for all categories. Each entry in the upper left J -by- J matrix, except the null diagonal entries, gives the proportion of the site that transitions from category i to a different category j during the time interval $[Y_t, Y_{t+1}]$. Equation (3) computes the upper left J -by- J entries for the Flow matrix by using the entries from the raw transition matrix and the notation in Table 1, which applies to all equations in our article.

$$a_{tij} = \frac{\text{Area of transition from category } i \text{ to } j \text{ during } [Y_t, Y_{t+1}]}{\text{Total area of the study site}} = \frac{c_{tij}}{\sum_{i=1}^J \sum_{j=1}^J c_{tij}} \quad (3)$$

Figure 1a shows a raw transition matrix for three categories. The area, e.g., square meters, of land that transitions from category i at time t to category j at time $t + 1$ is represented by c_{ij} . Category i in the rows represents the losing category, while category j in the columns represents the gaining category. Figure 1b shows a Markov transition matrix for three categories. The proportion of category i that transitions to category j from time t to

Table 1. Mathematical notation.

J	Number of categories
i	Index for a category at the initial time of an interval
j	Index for a category at the final time of an interval
T	Number of time points
t	Index for the initial time point of interval $[Y_t, Y_{t+1}]$, where t ranges from 1 to $T - 1$
d	Index for the initial time point of the shortest interval
Y_t	Year at time point t
a_{tij}	Size of area that transitions from category i to category j during time interval $[Y_t, Y_{t+1}]$ expressed as a proportion of the study site
m_{tij}	The Markov conditional probability that a transition occurs from category i to category j based on a matrix derived from time t to $t+1$
c_{tij}	Size of the area that transitions from category i at time Y_t to category j at time Y_{t+1}
S_t	Annual change area during time interval $[Y_t, Y_{t+1}]$ expressed as a proportion of the study site
U	Uniform annual change area during time extent $[Y_1, Y_T]$ expressed as a proportion of the study site
R	Proportion of change that would need to be reallocated to different time interval(s) to achieve uniform change during time extent $[Y_1, Y_T]$
R_{\max}	Maximum hypothetical value of R given the duration of the shortest time interval $[Y_d, Y_{d+1}]$

	Category 1	Category 2	Category 3	
Category 1	C_{11}	C_{12}	C_{13}	(a)
Category 2	C_{21}	C_{22}	C_{23}	
Category 3	C_{31}	C_{32}	C_{33}	

	Category 1	Category 2	Category 3	Total	
Category 1	$\frac{C_{11}}{\sum_{j=1}^3 C_{1j}}$	$\frac{C_{12}}{\sum_{j=1}^3 C_{1j}}$	$\frac{C_{13}}{\sum_{j=1}^3 C_{1j}}$	1.00	(b)
Category 2	$\frac{C_{21}}{\sum_{j=1}^3 C_{2j}}$	$\frac{C_{22}}{\sum_{j=1}^3 C_{2j}}$	$\frac{C_{23}}{\sum_{j=1}^3 C_{2j}}$	1.00	
Category 3	$\frac{C_{31}}{\sum_{j=1}^3 C_{3j}}$	$\frac{C_{32}}{\sum_{j=1}^3 C_{3j}}$	$\frac{C_{33}}{\sum_{j=1}^3 C_{3j}}$	1.00	

	Category 1	Category 2	Category 3	Gross Losses	
Category 1		$\frac{C_{12}}{\sum_{i=1}^3 \sum_{j=1}^3 C_{ij}}$	$\frac{C_{13}}{\sum_{i=1}^3 \sum_{j=1}^3 C_{ij}}$	$\frac{C_{13} + C_{12}}{\sum_{i=1}^3 \sum_{j=1}^3 C_{ij}}$	(c)
Category 2	$\frac{C_{21}}{\sum_{i=1}^3 \sum_{j=1}^3 C_{ij}}$		$\frac{C_{23}}{\sum_{i=1}^3 \sum_{j=1}^3 C_{ij}}$	$\frac{C_{21} + C_{23}}{\sum_{i=1}^3 \sum_{j=1}^3 C_{ij}}$	
Category 3	$\frac{C_{31}}{\sum_{i=1}^3 \sum_{j=1}^3 C_{ij}}$	$\frac{C_{32}}{\sum_{i=1}^3 \sum_{j=1}^3 C_{ij}}$		$\frac{C_{31} + C_{32}}{\sum_{i=1}^3 \sum_{j=1}^3 C_{ij}}$	
Gross Gains	$\frac{C_{21} + C_{31}}{\sum_{i=1}^3 \sum_{j=1}^3 C_{ij}}$	$\frac{C_{12} + C_{32}}{\sum_{i=1}^3 \sum_{j=1}^3 C_{ij}}$	$\frac{C_{13} + C_{23}}{\sum_{i=1}^3 \sum_{j=1}^3 C_{ij}}$	$\sum_{i=1}^3 \left[\left(\sum_{j=1}^3 C_{ij} \right) - C_{ii} \right]$	

Figure 1. Format of (a) the raw area transition matrix, (b) Markov matrix, and (c) Flow matrix.

time $t + 1$ is in each cell. Each row in the Markov matrix sums to one by design. Figure 1c shows the Flow matrix for three categories. The proportion of the site that transitions from one category to another is denoted in each entry, except for $i = j$, in which case the values are empty, i.e., the Flow matrix excludes persistence. The right-most column of the Flow matrix gives the gross losses of each category, while the bottom row gives the gross gains.

2.2. Calculating temporal instability using the Flow matrix

Equations (4) and (5) provide the mathematical basis for calculating our measure of temporal instability, R , in Equation (6). Equation (4) defines the annual proportion of the landscape that changes during each time interval $[Y_t, Y_{t+1}]$. Equation (5) defines the uniform annual proportion of the landscape that changes during the temporal extent $[Y_1, Y_T]$, which is the annual change that would be observed across the entire time series if change was perfectly stable during the time extent (Aldwaik and Pontius, in press).

$$S_t = \frac{\text{Proportion of site that transitions during } [Y_t, Y_{t+1}]}{\text{Duration of interval } [Y_t, Y_{t+1}]} = \frac{\left\{ \sum_{j=1}^J \left[\left(\sum_{i=1}^J a_{tij} \right) - a_{tjj} \right] \right\}}{(Y_{t+1} - Y_t)} \quad (4)$$

$$\begin{aligned}
 U &= \frac{\text{Sum of proportions of site that transitions during all intervals}}{\text{Sum of durations of all intervals}} \\
 &= \frac{\sum_{t=1}^{T-1} \left\{ \sum_{j=1}^J \left[\left(\sum_{i=1}^J a_{tij} \right) - a_{tjj} \right] \right\}}{(Y_T - Y_1)}
 \end{aligned} \tag{5}$$

Equation (6) calculates R , which is the proportion of change that would have to be reallocated to different time intervals in order for change to be perfectly stable. Equation (6) computes this by summing, for each interval, the duration of the interval multiplied by the maximum of either 0 or the difference between the annual change and the uniform annual change. Equation (6) produces one value that measures the proportion of change that is unstable across time extent $[Y_1, Y_T]$. If change was perfectly stable, then R would be zero. R increases as change becomes more unstable.

$$R = \frac{\sum_{t=1}^{T-1} \{ \text{MAXIMUM}[0, (S_t - U)] * (Y_{t+1} - Y_t) \}}{U * (Y_T - Y_1)} \tag{6}$$

For a given set of time intervals, the maximum possible value of R that could be observed is constrained by the shortest interval relative to the entire time extent. R_{\max} portrays a situation where all changes occur during the shortest time interval and no change occurs in any other time intervals. Equation (7) computes this maximum and the Appendix gives a mathematical proof.

$$R_{\max} = 1 - \frac{Y_{d+1} - Y_d}{Y_T - Y_1} \tag{7}$$

R_{\max} allows the user to determine the potential influence of time partitioning on R . If a site's time extent consists of exactly two intervals that are perfectly equal in duration, then R_{\max} is 0.5. As the duration of the shortest time interval shrinks, R_{\max} approaches 1, but can never equal 1. The minimum R value is zero, regardless of the length of the time intervals. R_{\max} is the saturation point of the measurement R for each site. Given a set of time intervals, R_{\max} is the maximum R value.

2.3. Data for case study: 10 LTER sites

The US National Science Foundation's Long Term Ecological Research (LTER) Network is a program of 26 sites, of which 10 contributed land-cover datasets from three or more time points to the Maps and Locals initiative (LTER 2010, MALS 2010). Figure 2 shows the site locations and Table 2 gives the characteristics of each site's data. These 10 sites represent a wide variety of biomes, temporal records, and data types. Dominant land-cover types include, from most to least common throughout the MALS network: forest, marsh, grassland, shrubland, pasture, cropland, and desert. The temporal extents at these sites range from 12 years for the Florida Coastal Ecosystems (FCE) to 100 years for Hubbard Brook (HBR). Figures 3–5 provide maps of each site in which darker shades indicate more frequent transitions over time. In these figures, a zero in the legend indicates persistence across the time extent. The maximum value for any pixel in these maps is equal to the number of time intervals.

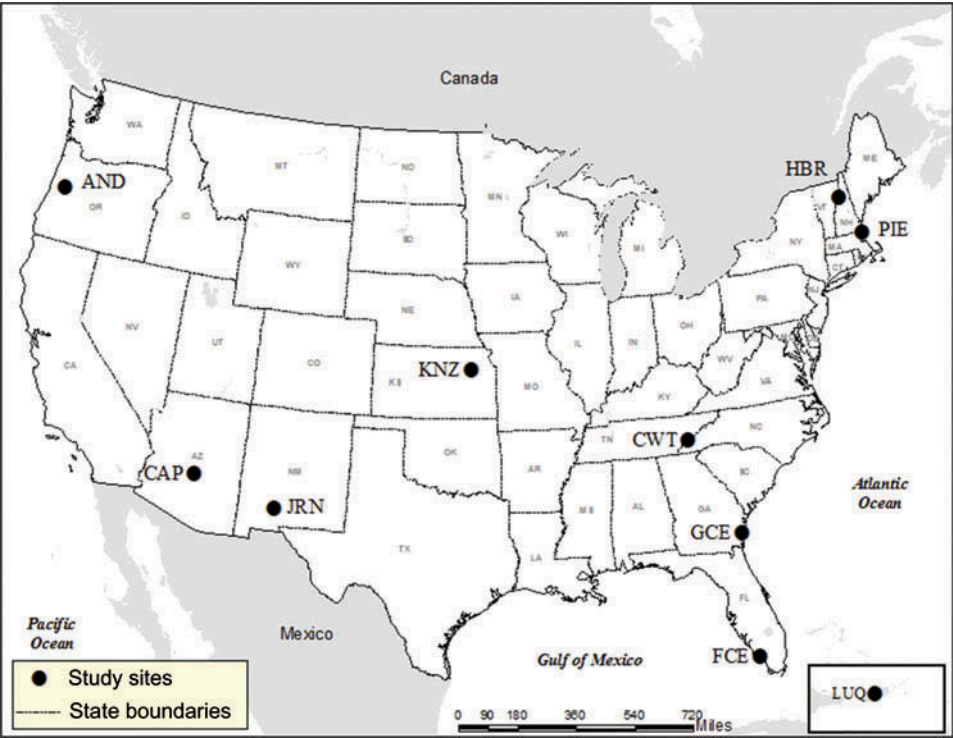


Figure 2. Location of 10 sites of the Maps and Locals (MALS) network.

Table 2. Descriptions of the 10 sites' data.

Site name (abbreviation)	Primary land cover(s)	Years of maps	Data resolution (m)	Number of categories
Luquillo (LUQ)	Pasture, Forest	1977, 1991, 2000	30	10
Coweeta (CWT)	Forest	1986, 1991, 1996	30	15
Plum Island Ecosystems (PIE)	Forest, Wetland	1971, 1985, 1991, 1999	30	7
Florida Coastal Ecosystems (FCE)	Freshwater Marsh	1994, 2001, 2006	200	8
Georgia Coastal Ecosystems (GCE)	Forested Wetland	1974, 1985, 1991, 2001, 2005	30	12
Hubbard Brook (HBR)	Forest	1860, 1930, 2001	30	2
Central Arizona/Phoenix (CAP)	Desert	1912, 1934, 1955, 1975, 1995	100	3
Konza (KNZ)	Grassland, Cropland	1990, 2005, 2009	30	6
Jornada (JRN)	Grassland, Shrubland	1915, 1928, 1998	100	12
Andrews (AND)	Coniferous Forest	1938, 1992, 2001	30	8

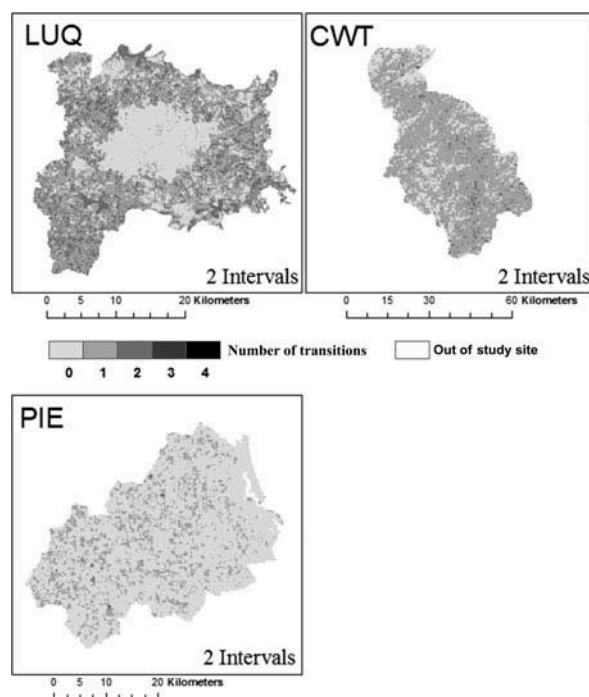


Figure 3. Maps of the most stable sites in this study. Darker shades indicate more frequent transitions at that pixel over the entire time extent.

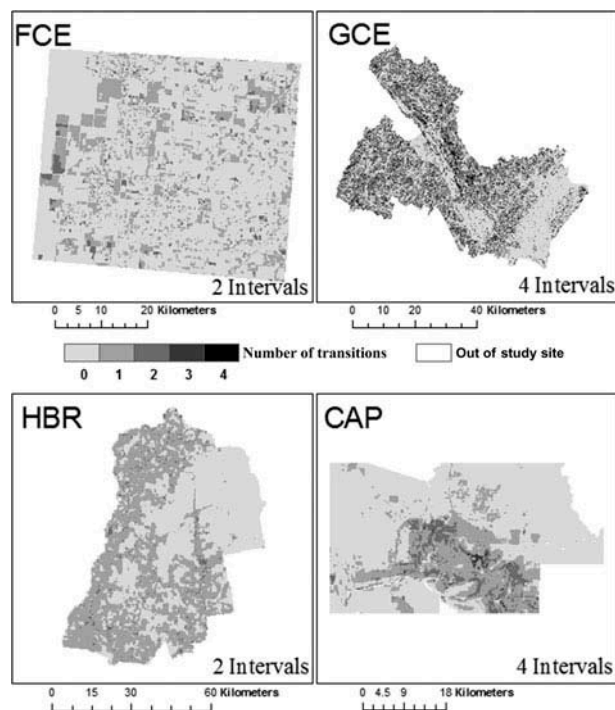


Figure 4. Maps of the four sites with mid-ranked instability. Darker shades indicate more frequent transitions at that pixel over the entire time extent.

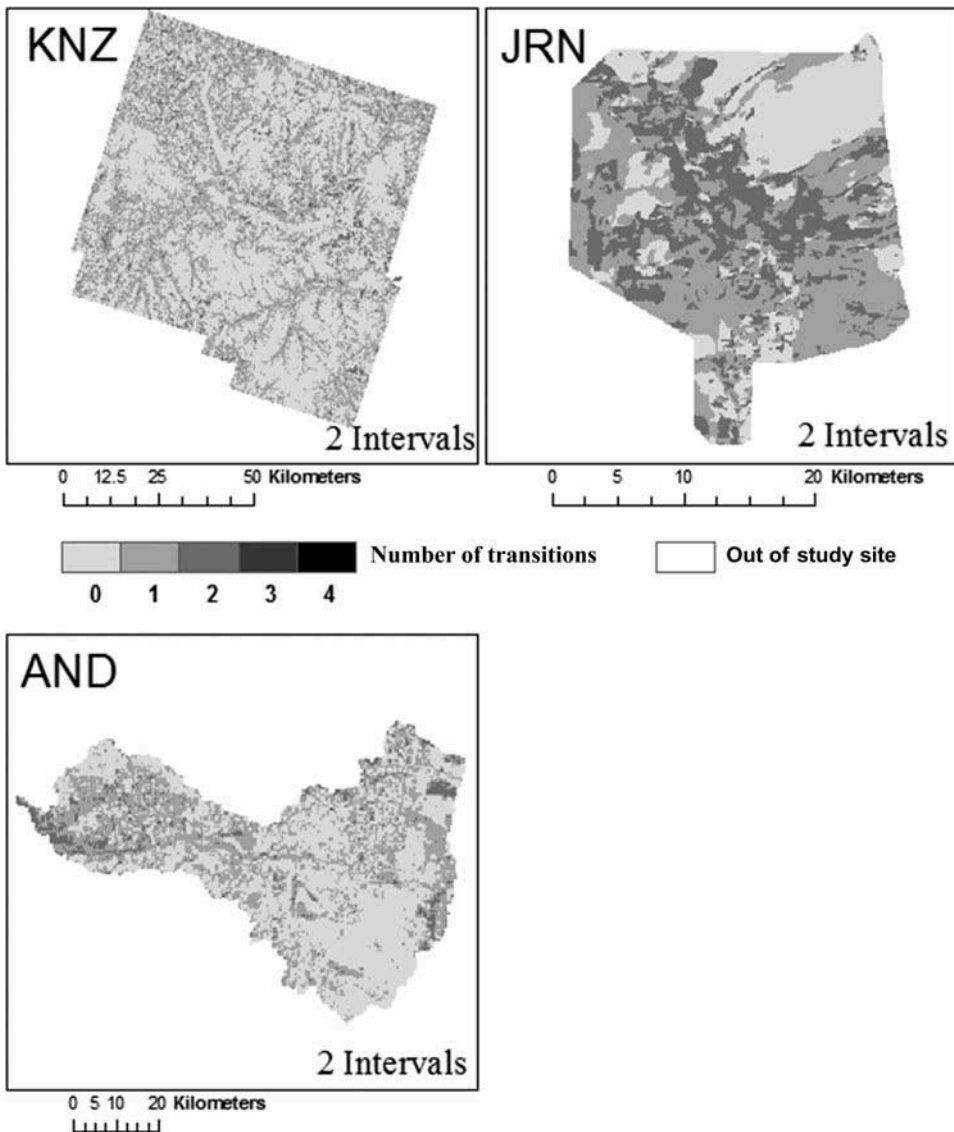


Figure 5. Maps of the four sites with the most instability. Darker shades indicate more frequent transitions at that pixel over the entire time extent.

3. Results

Figures 6–8 show the annual landscape change metrics S_t and U for each site, i.e., the results of Equations (4) and (5). The vertical axis is the annual change in the percent of the site. The horizontal axis is time. The area of each bar represents the proportion of the site that changed during interval $[Y_t, Y_{t+1}]$ because the width of each bar represents each interval's duration and the height of the bar represents the annual area of change S_t calculated in Equation (4). The solid horizontal line shows U , i.e., the uniform annual change during extent $[Y_1, Y_T]$.

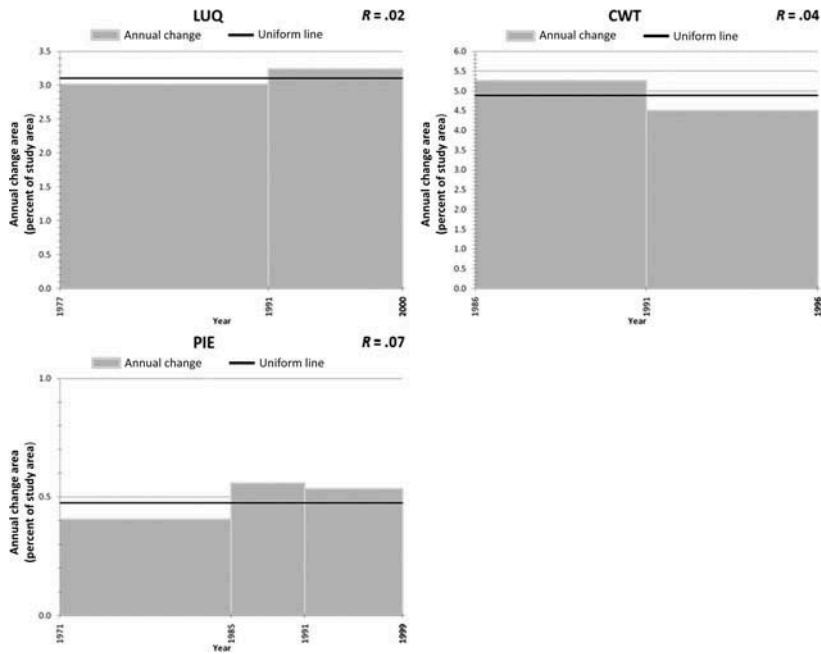


Figure 6. The annual change by time interval compared to the uniform annual change for sites with a percent of change that is unstable (R) less than 10.

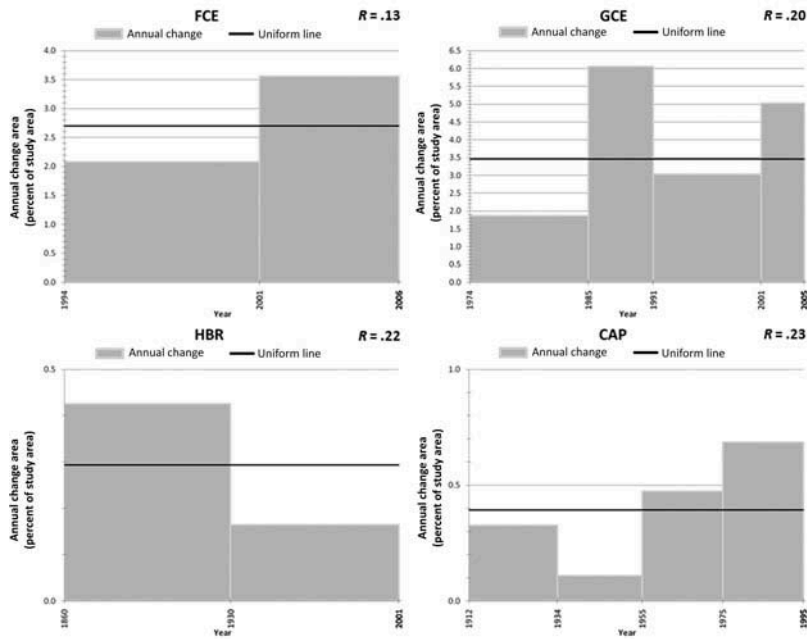


Figure 7. The annual change by time interval compared to the uniform annual change for sites with a percent of change that is unstable (R) from 10 to 25.

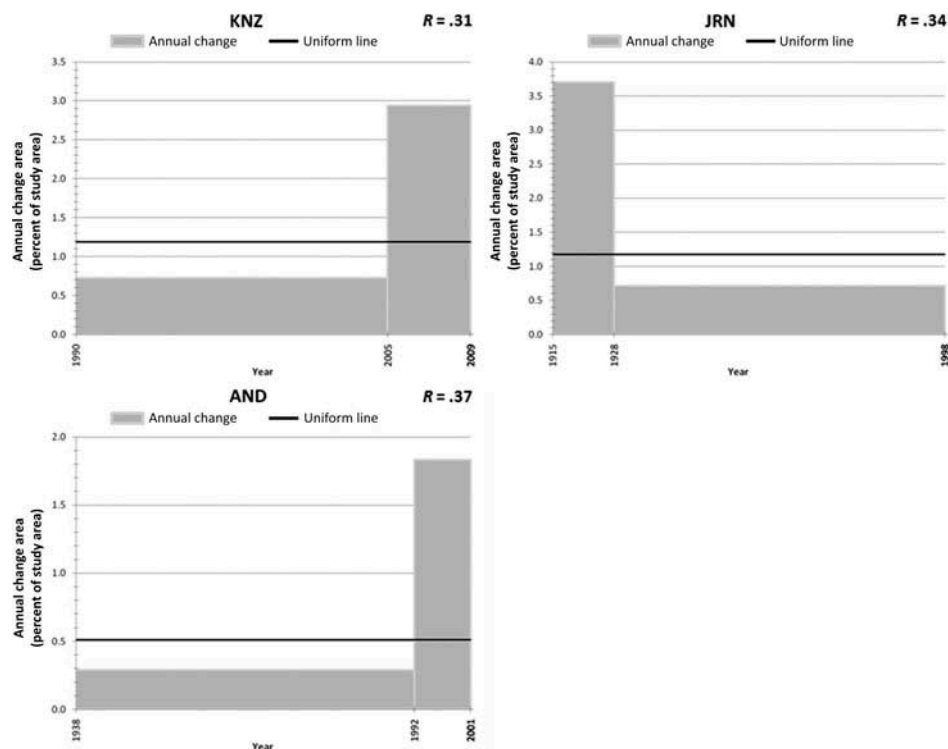


Figure 8. The annual change by time interval compared to the uniform annual change for sites with a percent of change that is unstable (R) greater than 25.

Luquillo (LUQ) and Coweeta (CWT) are relatively stable in terms of annual change across their time intervals. Konza (KNZ), Jornada (JRN), and Andrews (AND) each have a relatively short interval of fast change alongside a longer interval of slower change. The remaining study sites, such as FCE, Central Arizona/Phoenix (CAP), HBR, Georgia Coastal Ecosystems (GCE), and Plum Island Ecosystems (PIE), fall in between these two extremes.

Figure 9 shows R for all 10 sites. Each bar shows the measure of unstable change R as computed in Equation (6) multiplied by 100, to give the percent of change that is unstable. The saturation point R_{\max} is represented by a solid, horizontal black dash for each site.

4. Discussion

4.1. Applications of the metric R

4.1.1. Extrapolation

The metric R indicates how unstable land change has been, given the temporal extent and the time points that define each interval. The analysis identifies anomalies and their magnitudes relative to the time series. The method can help to test an assumption inherent to some empirical land change models: that past trends are appropriate to calibrate extrapolations into the future. Awareness of the level of historic instability can help in guiding the researcher to select or reject particular calibration intervals. If historic trends are

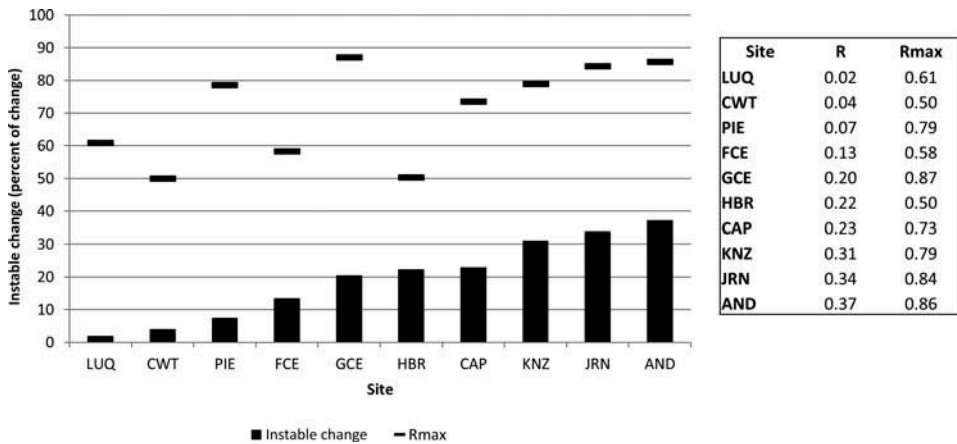


Figure 9. Percent of change that is unstable for each of the 10 MALS sites.

unstable, then each possible calibration interval could have a profoundly different influence on the extrapolation. For these unstable cases, further analysis is necessary to determine the interval that is most representative of the underlying processes of interest.

This has implications for the creation of scenarios, such as a business-as-usual scenario, which extrapolates historic trends. If historic trends are not stable, then it does not make sense to extrapolate a business-as-usual scenario. Measurement of historic instability could give some guidance regarding how to design scenarios of future land change. Of the 10 study areas analyzed, AND, KNZ, and JRN had the largest R values. Each study area had a long interval of slow annual change and a shorter interval of fast change. In other words, business has not been usual, and so scenarios that project past trends into the future would produce extrapolations that may not be meaningful. Conversely, any calibration interval would produce similar business-as-usual scenarios for sites such as LUQ or CWT.

4.1.2. Case examples

Table 3 gives and interprets R for a convenience sample of seven other published case studies. In the selection of papers, computation of R is useful for three distinct reasons. First, our method provides corroborating evidence that land-cover change is not stable over time in the cases of Shoyoma and Braimoh (2011), Muller and Middleton (1994), Mertens and Lambin (2000), Pelorosso et al. (2011), and Azocar et al. (2007). These five papers also illustrate the second reason that R provides a measurement of how unstable change is. Third, our method can give guidance regarding how to select a time interval to use as a reference for further work, as illustrated by data published in Cabezas *et al.* (2008). In their work, they suggest the use of a single duration (1927–1957) as a reference for the ‘more natural functioning of the river–floodplain system’ (p. 2773). However, the two intervals within this duration (1927–1946 and 1946–1957) are relatively unstable ($R = 0.25$). This leaves the reader to wonder which part of the time extent is appropriate for the use as a reference.

4.1.3. Additional applications

Our approach takes steps toward providing an analysis of the temporal resolution(s) at which phenomena are stable. For example, deforestation and reforestation occur cyclically

Table 3. Application of the method described in this article to matrices in other articles.

Authors (year)	Authors' conclusion	Time points	$R(R_{\max})$	Interpretation of R
Wang <i>et al.</i> (2009)	'soil erosion in Xingguo County experienced three pronounced phases during the study periods.' p. 313	1958 1975 1982 2000	0.03 (0.83)	R shows that annual change in Xingguo County was fairly stable over the temporal extent.
Shoyama and Braimoh (2011)	Different stages of land change are reflected in three time intervals	1947 1968 1978 2004	0.14 (0.82)	R provides additional evidence that the three intervals are unstable, i.e., that annual change occurred differently within the time extent. Their study area could be characterized as moderately stable relative to the other study areas in our article.
Muller and Middleton (1994)	'The hypothetical equilibrium is based on the unrealistic assumption that the transition matrix remains constant, i.e., land-use change is constant.' p. 154	1936 1952 1965 1976 1981	0.14 (0.89)	We agree with Muller and Middleton's conclusion. R provides information on the degree of nonstationarity in their data. Their case study is moderately stable relative to the sites shown in Figure 9.
Mertens and Lambin (2000)	'The transition matrix is nonstationary' p. 481	1973 1986 1991 1996	0.18 (0.78)	We agree with Mertens and Lambin's conclusion. In this case, our equation provides support for their conclusion and provides an efficient measurement of the nonstationarity of annual change among intervals. R provides information on the degree of nonstationarity.

(Continued)

Table 3. (Continued).

Authors (year)	Authors' conclusion	Time points	$R(R_{\max})$	Interpretation of R
Pelorosso <i>et al.</i> (2011)	'The land-cover change process in Micigliano is not stationary' p. 342	1954 1985 1999	0.21 (0.69)	We agree with Pelorosso <i>et al.</i> that the land-cover change process is not stationary. R is consistent with the findings of a more complex approach to measuring Markov chain's temporal stability, the Anderson–Goodman test.
Cabezas <i>et al.</i> (2008)	'The ecotope structure and dynamics of the 1927–1957 [interval] should be adopted as the guiding image' p. 2760	1927 1946 1957	0.25 (0.63)	Cabezas <i>et al.</i> suggest that 1927–1957 would be helpful to adopt as a 'guiding image', but change within that interval is relatively unstable. This indicates that a more specific interval should be chosen.
Azocar <i>et al.</i> (2007)	Different urban policies in Los Angeles are reflected in change after 1978	1955 1978 1992 1998	0.30 (0.62)	R suggests that change was highly unstable from 1955 to 1998. R gives further evidence for the authors' conclusion.

over the intervals provided by the GCE. If these cycles are measured with a coarse temporal resolution, then the process appears stable. Conversely, if these cycles are measured with a fine temporal resolution, then the phenomenon appears unstable. If one has data from multiple time points, then the calculation of R at variable temporal resolutions can help to identify the temporal resolution at which land change is stable. This can give researchers guidance on the appropriate temporal resolution to examine their phenomenon of interest.

Figure 10 illustrates how to identify the temporal resolution at which the change is stable, using an example from the GCE LTER. Within GCE, there is a cyclical pattern of deforestation and reforestation. At the original temporal resolution of the data seen in Figure 10a, the cyclical pattern of change is captured, suggesting that change in GCE is fairly unstable over shorter time durations. However, the cyclical pattern of change is canceled when the temporal resolution of the data is coarsened, suggesting that change in GCE is fairly stable over longer time durations (see Figure 10b). This canceling can occur when transitions in one interval are reversed in a subsequent interval. For example, if an area converts from forest to bare soil during one interval, and then back to forest during the subsequent interval, then it appears as forest persistence when the two consecutive intervals are aggregated (also see Aldwaik and Pontius 2013). Further, Figure 10c shows an example when interval aggregation causes change to become more unstable, since the majority of change occurs during the last time interval. While Figures 10a and c have an

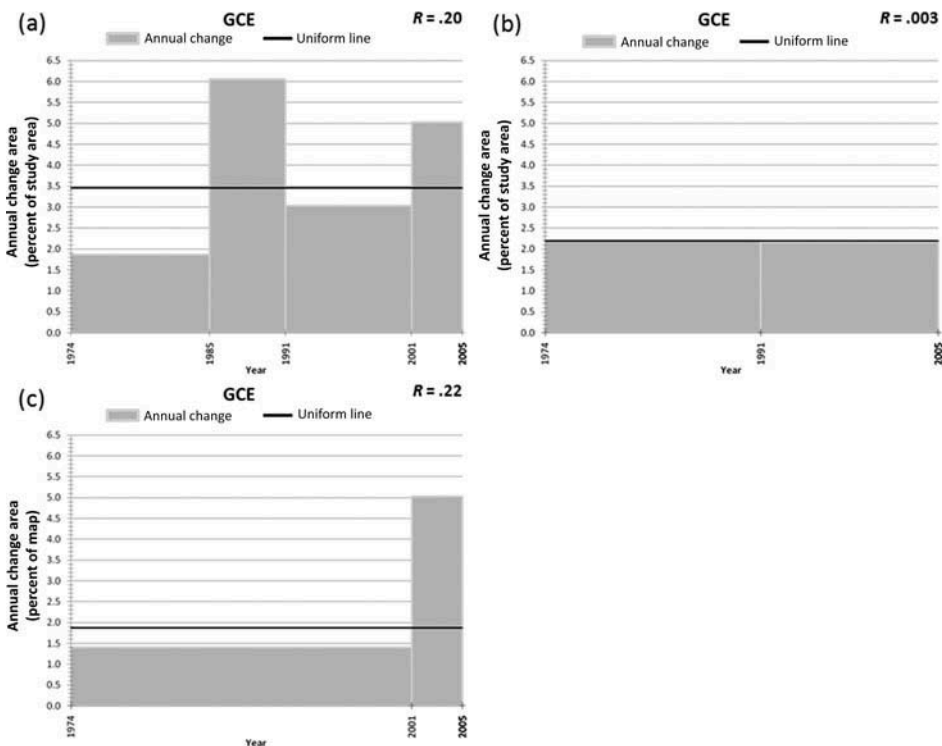


Figure 10. Example of how the temporal resolution of data can influence the analysis of temporal stability, where (a) shows five time points, (b) shows three time points selected to illustrate temporal stability, and (c) shows three time points selected to illustrate temporal instability.

identical R_{\max} , the finer temporal resolution of Figure 10a shows a more stable pattern than the coarser resolution in Figure 10c.

Aggregation of time intervals can help to identify the temporal resolution that is appropriate to analyze. In the GCE case, if the researcher is interested in the impacts of forest management strategies on the long-term quantity of forest, then a coarser temporal resolution might be more appropriate to avoid the variation caused by short-term cyclical changes. However, if a researcher is interested in the influence of land change on animal populations, then a fine temporal resolution would be more appropriate because coarse resolutions may not capture details that are important to animals, such as landscape persistence.

4.2. Considerations for application of the metric R

4.2.1. Characteristics of the measurement of R

The definition of R uses a Flow matrix for the calculation of the annual change. We opt to use the Flow matrix for many reasons. The Flow matrix assumes linear change with respect to time during each time interval. The Markov matrix assumes nonlinear change with respect to time because the Markov matrix assumes a constant proportion change of the base during each time step. These approaches make different assumptions regarding how systems function. When the Flow matrix is used for extrapolation, classes can be driven to zero, i.e., a class can be completely removed from the landscape. When the Markov matrix is used for extrapolation, all classes remain present as they reach equilibrium, even though they might approach zero. There are also practical reasons for selecting the Flow matrix over the Markov matrix. It is straightforward to convert the Flow matrix for an interval to an annualized Flow matrix by dividing each entry by the number of years within the interval. It is not straightforward to convert a Markov matrix for an interval to an arbitrary time step, since there might be multiple solutions or no solutions that give probabilities between 0 and 1 (Takada *et al.* 2010).

Another characteristic of the measurement R is that it ignores the sequential ordering of time intervals. A study site that has one interval of fast change followed by two intervals of slow change would have the same R as a study site with one interval of fast change between two intervals of slow change. For example, KNZ and AND have a long interval of slow change followed by a short interval of fast change. JRN has a short interval of fast change followed by a long interval of slow change. Figure 9 shows that all three of these study sites have a similar R value despite this difference.

4.2.2. Considerations for the use of the metric R

There are important caveats for methods that use the raw transition matrix, and many of these caveats apply to R . First, the temporal extent and the number of time intervals are frequently determined by data availability, rather than knowledge of the phenomena of interest. In the current state of data availability, we expect our method will be used frequently to test whether the process of interest is stable among the available time points, rather than exploring multiple intervals to determine at which temporal resolution stability exists. If data are available for multiple years, then our method can be used to examine how instability varies as a function of time intervals, as Figure 10 illustrates. We expect this type of exploratory analysis will be more achievable in the near future, as many remote sensing programs are adopting policies that allow free access to satellite imagery, e.g., the

US Landsat, China and Brazil's China–Brazil Earth Resources Satellite (CBERS), and the European Space Agency's Sentinel-2.

A second caveat is that R does not account for possible errors in the maps. Our article does not discuss error in depth because many recent studies have addressed the topic of how map error can influence measurement of landscape change (Stow 1990, 1999, Pontius and Lippitt 2006, Stehman and Wickham 2006, Pontius and Li 2010, Aldwaik and Pontius in this issue). However, R may be able to expose the nature of errors and inconsistencies in the data. If a particular time interval has a much different annual change compared to other intervals, then researchers should investigate whether the maps that bound the interval have errors or whether the maps were produced following different methodologies.

A third caveat is that the maximum value of R is dependent on the shortest time interval, as Figure 11 illustrates. This feature of Equation (7) is related to the temporal resolution of the data. As finer temporal resolutions are acquired, it is possible to see more detailed measurements of sudden changes, i.e., shocks.

The metric R must additionally be interpreted in the context of both the categorical and spatial resolution of data at each site. Different categorical schemes can result in dramatically different observations of change at a site (Aldwaik and Pontius, in press CEUS), and so comparisons must be made in the context of the given scheme. Similarly, spatial resolution can influence the quantity of observed change (Pontius and Connors 2009).

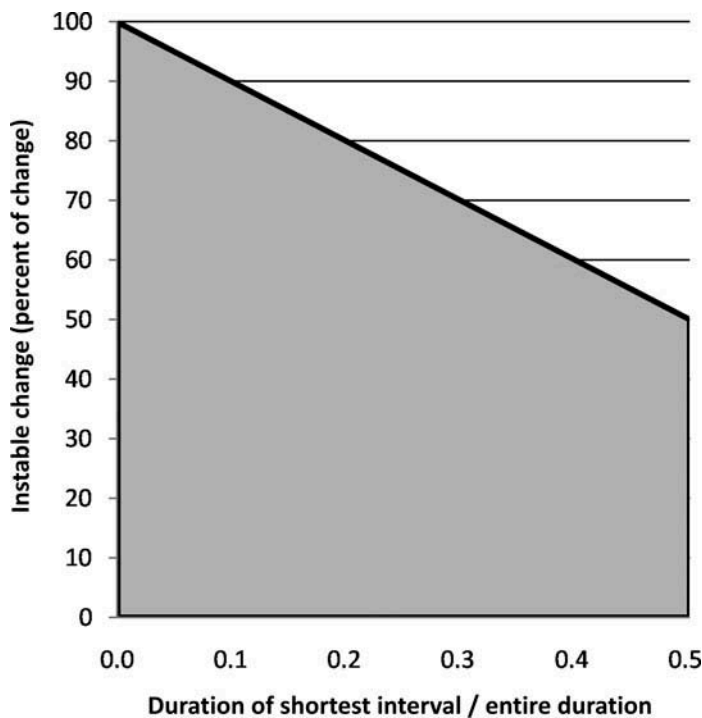


Figure 11. Mathematically possible region for R as a function of the duration of the shortest interval divided by the duration of the temporal extent. See Equation (7).

4.3. Future research

A number of fruitful research directions exist to understand the temporal stability of land changes. Our next research goal is to produce a variant of R that is less sensitive to the intervals' durations. This might improve the ability of researchers to understand the characteristics of the processes driving land change. It would facilitate comparative studies, as well as to take a step toward adapting this method for the use with deductive modeling frameworks.

It would be possible to compute R using any entry in the Flow matrix. This can be characterized into three levels of analysis: interval (as presented in our article), category (tabular gross losses and gains for each category), and transition (individual c_{ij} transitions) (Aldwaik and Pontius, in this issue). Categorical and transition level analysis could be useful for researchers seeking to understand cyclical changes of specific land-cover categories, or to refine the interval level analysis to better understand the underlying drivers of instability.

Our work questions the utility of exclusively employing the Markov matrix for land change analysis. The Markov matrix has had a great deal of influence on the design of land-change models, but the Markov matrix has not been compared with the alternative matrices, such as the Flow matrix. It is critical that the properties of different matrices are understood and compared so that researchers can choose the most appropriate matrix for their needs, goals, and assumptions.

Data-intensive scientific discovery is becoming the so-called fourth paradigm for research (Hey *et al.* 2009); thus, it is important to examine applications of the Flow matrix to increasingly large datasets. With very large data products, e.g., daily drought classifications, it would likely be possible to identify whether a system appears to be headed toward a tipping point. This knowledge could be used to create an early warning indicator regarding whether a system-altering transition is imminent (Carpenter and Brock 2006, Scheffer *et al.* 2009). Additionally, our method could be employed to search for and to characterize drivers of change, in terms of both the stability and timing with which drivers operate.

Finally, R could potentially be used to identify instability in phenomena other than land change. For example, one could assess instability where time points are elections, elements are political offices, and categories are political parties who occupy the offices. Our article's concepts could apply also to a continuous variable, such as a patient's weight recorded across multiple doctor visits.

5. Conclusions

This article presents a method to analyze maps of land categories at more than two time points. The metric R measures the proportion of change that would need to be reallocated to different time intervals to achieve uniform annual change across a site's temporal extent. The article illustrates the method by computing R for 10 sites with varying biomes, extents, and data types. Our article also computes and interprets R for a convenience sample of published land-change data.

This measurement of the instability of land change (R) is influenced by the temporal extent, the temporal interval durations, and the annual change during each interval. Of the 10 sites analyzed, AND, KNZ, and JRN had the largest R value. Each of these three sites had an extended interval of slow change and a shorter interval of fast change. Under these circumstances, it makes little sense to extrapolate a business-as-usual scenario from the

available data because these data show that business has not been usual. Conversely, LUQ and CWT had the lowest R values among the analyzed sites.

Current land-change models are hampered by a limited knowledge of the historical precedence for events. This article mitigates this concern by (1) introducing the Flow matrix, (2) providing a framework to measure historical instability, (3) characterizing the behavior of our measurement, (4) providing examples from sites that have a variety of characteristics, and (5) discussing the implications of different types of temporal instability and how they could influence land change analyses.

Acknowledgements

The United States' National Science Foundation (NSF) supported this work via the following programs: Long Term Ecological Research via grants OCE-0423565 & OCE-1058747 for Plum Island Ecosystems and OCE-0620959 for Georgia Coastal Ecosystems, Coupled Natural Human Systems via grant BCS-0709685, Research Experiences for Undergraduates via grant SES-0849985, and Urban Long Term Research Areas via grant BCS-0948984. The NSF supplied additional funding through a supplement grant entitled "Maps and Locals (MALS)" via grant DEB-0620579. The work has also benefited from the NICHD funded University of Colorado Population Center (grant R21 HD51146) for research, administrative, and computing support. Any opinions, findings, conclusions, or recommendation expressed in this paper are those of the authors and do not necessarily reflect those of the funders. Anonymous reviewers supplied constructive feedback that helped to improve this paper.

References

- Aldwaik, S.Z. and Pontius Jr., R.G., 2013. Map errors that could account for deviations from a uniform intensity of land change. *International Journal of Geographic Information Science*, in press.
- Aldwaik, S.Z. and Pontius Jr., R.G., in press. Sequential land category aggregations to maintain maximum change over time. *Computers, Environment and Urban Systems*.
- Aldwaik, S.Z. and Pontius Jr., R.G., 2012. Intensity analysis to unify measurements of size and stationarity of land changes by interval, category, and transition. *Landscape and Urban Planning*, 106, 103–114.
- Alo, C. and Pontius Jr., R.G., 2008. Identifying systematic land-cover transitions using remote sensing and GIS: the fate of forests inside and outside protected areas of Southwestern Ghana. *Environment and Planning B: Planning and Design*, 35 (2), 280–295.
- An, L. and Brown, D., 2008. Survival analysis in land change science: integrating with GIScience to address temporal complexities. *Annals of the Association of American Geographers*, 98 (2), 323–344.
- Azocar, G., et al., 2007. Urbanization patterns and their impacts on social restructuring of urban space in Chilean mid-cities: the case of Los Angeles, Central Chile. *Land Use Policy*, 24 (1), 199–211.
- Bell, E. and Hinojosa, R., 1977. Markov analysis of land use change: continuous time and stationary processes. *Socio-Economic Planning Sciences*, 11 (1), 13–17.
- Braimoh, A., 2006. Random and systematic land-cover transitions in northern Ghana. *Agriculture, Ecosystems & Environment*, 113 (1–4), 254–263.
- Cabezas, A., et al., 2008. Hydrologic and land-use change influence landscape diversity in the Ebro River (NE Spain). *Landscape*, 5, 2759–2789.
- Caillault, S., et al., in press. Influence of inventive networks on landscape changes: a simple agent-based simulation approach. *Environmental Modeling and Software*. Available from: <http://dx.doi.org/10.1016/j.envsoft.2012.11.003>.
- Carpenter, S. and Brock, W. (2006). Rising variance: a leading indicator of ecological transition. *Ecology Letters* 9, 311–318.
- Ellis, D.G., 1979. Relational control in two group systems. *Communications Monographs*, 46 (3), 153–166.

- Flamenco-Sandoval, A., Martínez Ramos, M., and Masera, O.R., 2007. Assessing implications of land-use and land-cover change dynamics for conservation of a highly diverse tropical rain forest. *Biological Conservation*, 138 (1–2), 131–145.
- Foley, J., *et al.*, 2005. Global consequences of land use. *Science*, 309 (5734), 570.
- GLP, 2010. *Theme 2: consequences of land system change feedbacks to the coupled earth*. Copenhagen: GLP International Project Office.
- Goodman, A.L. and Anderson, W., 1957. Statistical inference about Markov chains. *The Annals of Mathematical Statistics*, 28, 89–110.
- Hey, A.J.G., Tansley, S., and Tolle, K.M. 2009. *The fourth paradigm: data-intensive scientific discovery*. Washington: Microsoft Research.
- Lambin, E., 1997. Modelling and monitoring land-cover change processes in tropical regions. *Progress in Physical Geography*, 21 (3), 375.
- Lambin, E., *et al.*, 2001. The causes of land-use and land-cover change: moving beyond the myths. *Global Environmental Change*, 11 (4), 261–269.
- Mertens, B. and Lambin, E.F., 2000. Land-cover-change trajectories in southern Cameroon. *Annals of the Association of American Geographers*, 90 (3), 467–494.
- Muller, M.R. and Middleton, J., 1994. A Markov model of land-use change dynamics in the Niagara Region, Ontario, Canada. *Landscape Ecology*, 9 (2), 151–157.
- Nagendra, H., Munroe, D., and Southworth, J., 2004. From pattern to process: landscape fragmentation and the analysis of land use/land cover change. *Agriculture, Ecosystems and Environment*, 101 (2–3), 111–115.
- Parker, D.C., *et al.*, 2003. Multi-agent systems for the simulation of land-use and land-cover change: a review. *Annals of the Association of American Geographers*, 93 (2), 314–337.
- Pelorusso, R., *et al.*, 2011. Stability analysis for defining management strategies in abandoned mountain landscapes of the Mediterranean basin. *Landscape and Urban Planning*, 103 (3), 335–346.
- Petit, C., Scudder, T., and Lambin, E., 2001. Quantifying processes of land-cover change by remote sensing: resettlement and rapid land-cover changes in south-eastern Zambia. *International Journal of Remote Sensing*, 22 (17), 3435–3456.
- Pontius Jr., R.G. and Connors, J., 2009. Range of categorical associations for comparison of maps with mixed pixels. *Photogrammetric Engineering & Remote Sensing*, 75 (8): 963–969.
- Pontius, R.G. Jr. and Li, X., 2010. Land transition estimates from erroneous maps. *Journal of Land Use Science*, 5 (1), 31–44.
- Pontius, R. G. Jr. and Lippitt, C., 2006. Can error explain map differences over time? *Cartography and Geographic Information Science*, 33 (2), 159–171.
- Pontius Jr., R.G. and Neeti, N., 2010. Uncertainty in the difference between maps of future land change scenarios. *Sustainability Science*, 5 (1), 39–50.
- Pontius Jr., R.G., Shusas, E., and McEachern, M., 2004. Detecting important categorical land changes while accounting for persistence. *Agriculture, Ecosystems and Environment*, 101 (2–3), 251–268.
- Pontius Jr., R.G., *et al.*, 2007. Accuracy assessment for a simulation model of Amazonian deforestation. *Annals of the Association of American Geographers*, 97 (4), 677–695.
- Pueyo, Y. and Beguería, S., 2007. Modelling the rate of secondary succession after farmland abandonment in a Mediterranean mountain area. *Landscape and Urban Planning*, 83 (4), 245–254.
- Rindfuss, R., *et al.*, 2004. Developing a science of land change: challenges and methodological issues. *Proceedings of the National Academy of Sciences of the United States of America*, 101 (39), 13976–13981.
- Scheffer, M., *et al.*, 2009. Early-warning signals for critical transitions. *Nature*, 461, 53–59.
- Shoyama, K. and Braimoh, A., 2011. Analyzing about sixty years of land-cover change and associated landscape fragmentation in Shiretoko Peninsula, Northern Japan. *Landscape and Urban Planning*, 101 (1), 22–29.
- Stehman, S.V. and Wickham, J.D., 2006. Assessing accuracy of net change derived from land cover maps. *Photogrammetric Engineering and Remote Sensing*, 72 (2), 175.
- Stow, D., 1990. Land use change detection based on multi-date imagery from different satellite sensor systems. *Geocarto International*, 5 (3), 3–12.
- Stow, D., 1999. Reducing the effects of misregistration on pixel-level change detection. *International Journal of Remote Sensing*, 20 (12), 2477–2483.

- Takada, T., Miyamoto, A., and Hasegawa, S., 2010. Derivation of a yearly transition probability matrix for land-use dynamics and its applications. *Landscape Ecology*, 25 (4), 561–572.
- Turner, B.L., *et al.*, 1995. *HDP report No. 07: land-use and land-cover change science/research plan*. Stockholm: Human Dimensions of Global Environmental Change Programme (HDP).
- UN-REDD, 2010. *The United Nations Collaborative Programme on Reducing Emissions from Deforestation and Forest Degradation in Developing Countries* [online]. United Nations. Available from: <http://www.un-redd.org/> [Accessed 21 April 2013].
- Versace, V., *et al.*, 2008. Appraisal of random and systematic land cover transitions for regional water balance and revegetation strategies. *Agriculture, Ecosystems & Environment*, 123 (4), 328–336.
- Wang, K., *et al.*, 2009. Landscape analysis of dynamic soil erosion in Subtropical China: a case study in Xingguo County, Jiangxi Province. *Soil and Tillage Research*, 105 (2), 313–321.

Appendix

This is a mathematical proof of Equation (7), which defines R_{\max} . We use the notation defined in Section 2.1.

Let d denote the initial time of the interval with the shortest duration. If two or more intervals have the same shortest duration, then select one of the shortest intervals arbitrarily. Assume change occurs during the shortest interval, and no change occurs in any other time intervals. Let Δ denote the amount of change that occurs during the shortest interval. Equation (4) results in S_d below for the shortest interval and gives $S_i = 0$ for all other intervals.

$$S_d = \frac{\text{Proportion of change during the shortest interval}}{\text{Duration of the shortest interval}} = \frac{\Delta}{Y_{d+1} - Y_d}$$

Following the above assumptions, U resolves to

$$U = \frac{\text{Proportion of change during all intervals}}{\text{Sum of durations of all intervals}} = \frac{\Delta}{(Y_T - Y_1)}$$

Finally, R resolves to an expression that we define as R_{\max} :

$$\begin{aligned} R_{\max} &= \frac{\sum_{t=1}^{T-1} \{\text{MAX}[0, (S_t - U)] * (Y_{t+1} - Y_t)\}}{U * (Y_T - Y_1)} \\ &= \frac{\sum_{t=1}^{T-1} \left\{ \text{MAX} \left[0, \left(\frac{\Delta}{Y_{d+1} - Y_d} - \frac{\Delta}{Y_T - Y_1} \right) \right] * (Y_{t+1} - Y_t) \right\}}{\frac{\Delta}{Y_T - Y_1} * (Y_T - Y_1)} \\ &= \frac{\left(\frac{\Delta}{Y_{d+1} - Y_d} - \frac{\Delta}{Y_T - Y_1} \right) * (Y_{d+1} - Y_d)}{\Delta} \\ &= \left(\frac{1}{Y_{d+1} - Y_d} - \frac{1}{Y_T - Y_1} \right) * (Y_{d+1} - Y_d) \\ &= 1 - \frac{Y_{d+1} - Y_d}{Y_T - Y_1} \end{aligned}$$